Phagosomal Copper–promoted Oxidative Attack on Intracellular *Mycobacterium tuberculosis*

M. Daben J. Libardo[1], Cesar de la Fuente-Nuñez[2-4], Kushi Anand[5], Gopinath Krishnamoorthy[6], Peggy Kaiser[6], Stephanie C. Pringle[7], Christopher Dietz[1], Scott Pierce[1], Michael B. Smith[1], Amy Barczak[7,8,9], Stefan H.E. Kaufmann[6], Amit Singh[5,], and Alfredo M. Angeles-Boza[1,10,]**

[1]Department of Chemistry, University of Connecticut, 55 N. Eagleville Rd., Storrs, CT 06269, USA

[2]Synthetic Biology Group, MIT Synthetic Biology Center, Department of Biological Engineering, and Department of Electrical Engineering and Computer Science, Massachusetts Institute of Technology, 21 Ames St., Cambridge, MA 02139, USA

[3]Research Laboratory of Electronics, Massachusetts Institute of Technology, 50 Vassar St., Cambridge, MA 02139, USA

[4]The Broad Institute of MIT and Harvard, 415 Main St., Cambridge, MA 02139, USA

[5]Department of Microbiology and Cell Biology, Center for Infectious Disease Research, Indian Institute of Science, Bangalore 560012, India

[6]Department of Immunology, Max Planck Institute for Infection Biology, Virchowweg 12, Berlin 10117, Germany

[7]The Ragon Institute of Harvard, MIT, and Massachusetts General Hospital, 400 Technology Square, Cambridge, MA 02139, USA

[8]Division of Infectious Disease, Massachusetts General Hospital, 55 Fruit St., Boston, MA 02114, USA

[9]Department of Medicine, Harvard Medical School, 25 Shattuck St., Boston, MA 02115, USA

[10]Institute of Materials Science, University of Connecticut, 97 N. Eagleville Rd., Storrs, CT 06269, USA

*Correspondence: alfredo.angeles-boza@uconn.edu and asingh@iisc.ac.in

Copper (Cu) ions are critical in controlling bacterial infections, and successful pathogens like *Mycobacterium tuberculosis* (Mtb) possess multiple Cu resistance mechanisms. We report, as proof of concept, that a novel Cu hypersensitivity phenotype can be generated in mycobacteria, including Mtb, through a peptide, DAB-10, that is able to form reactive oxygen species (ROS) following Cu-binding. DAB-10 induces intramycobacterial oxidative stress in a Cu-dependent manner *in vitro* and during infection. DAB-10 penetrates murine macrophages and encounters intracellular mycobacteria. Significant intracellular Cu-dependent protection was observed when Mtb-infected macrophages were treated with DAB-10 alongside a cell-permeable Cu chelator. Treatment with the Cu chelator reversed the intramycobacterial oxidative shift induced by DAB-10. We conclude that DAB-10 utilizes the pool of phagosomal Cu ions in the host-Mtb interface to augment the mycobactericidal activity of macrophages while simultaneously exploiting the susceptibility of Mtb to ROS. DAB-10 serves as a model with which to develop next-generation, multi-functional antimicrobials.

KEYWORDS: antimicrobial, peptide, bioinorganic chemistry, mycobactericidal, copper binding

In 2016, more than 1.6 million deaths from tuberculosis (TB) were reported, with an estimated 10.4 million incident cases, making *Mycobacterium tuberculosis* (Mtb) the most lethal single infectious agent.[1] This problem is exacerbated by the alarming rate at which multidrug-resistant (MDR) and extensively drug-resistant (XDR) Mtb strains are emerging, which is extinguishing the efficacy of current anti-TB drugs. Therefore, there is an urgent need to develop therapeutics that target this pathogen in novel ways and a pressing demand to understand their mechanism of action. For TB, multiple strategies involving bacterial enzyme targeting[2] and modulation of host-immune response[3] were proven to be effective in proof-of-concept studies, whereas the exploration of agents that exploit factors at the host-pathogen interface has been limited. More specifically, capitalizing on transition metal trafficking in macrophages as a strategy to target TB has been suggested,[4] but has not been explored until now.

It is widely known that transition metal trafficking within primary macrophages is altered in response to infection. In keeping with the concept of nutritional immunity, iron and manganese are limited within the phagosomes to deprive pathogens of these essential micronutrients.[5, 6] On the other hand, as substrate to the transporter ATP7A, Cu is deliberately enriched in phagosomes and contributes to the microbicidal effect of macrophages.[7] Considering the redox cycling of Cu, its ability to displace metal cofactors of enzymes, its iron-sulfur cluster targeting, and its thiophilic nature,[8] it becomes apparent why reallocating this toxic metal to sites containing bacteria is advantageous. Indeed, the phagosomes of Mtb-infected macrophages contain 25 – 400 μM of Cu.[9] However, there exist redundant defense mechanisms that protect Mtb from Cu-related toxicity. The bacilli express CtpV and MctB, membrane-bound Cu efflux pumps that transport Cu back to the phagosomal lumen.[10, 11] In addition, Mtb expresses cytosolic metallothionein (MymT) which sequesters up to six Cu(I) ions,[12] and a periplasmic oxidase (MmcO) which converts Cu(I) to the less toxic Cu(II).[13] Together, these proteins form an arsenal of defenses that confer Mtb resistance towards phagosomal Cu stress.

The profusion of Cu ions at the host-Mtb interface therefore represents an axis that can be exploited for therapeutic purposes. Indeed, recent reports have shown that Mtb can be resensitized to Cu by using small molecule copper chelators like thiolated semicarbazones[14] and 8-hydroxyquinoline[15] that rely on a

Trojan horse strategy to increase intracellular Cu concentration; and disulfiram[16] that interfere with Cu homeostatic pathways. Together, these studies represent significant advances in developing Cu-dependent antimicrobials but fall short in demonstrating the efficacy of this strategy in an *ex vivo* model of infection.

While Mtb can withstand high Cu concentrations, it is extremely susceptible to endogenous increase in reactive oxygen species (ROS).[17] The pro-oxidant activity of ascorbic acid triggers the accumulation of hydroxylated fatty acids in the membrane leading to rapid sterilization of axenic cultures.[18] Moreover, ROS induced by bactericidal antibiotics and inhibitors of sulfur metabolism were demonstrated to be effective in eradicating nonreplicating mycobacteria, persisters, and drug resistant Mtb.[19-21] Reactive nitrogen species (RNS) liberated from intrabacterial reduction of PA-824 (a bicyclic nitroimidazole) and hydroquinone-based small molecules that generate superoxide radicals were shown to efficiently kill nonreplicating and drug-resistant Mtb.[17, 22] These studies suggest that ROS-forming compounds hold the potential to sterilize an Mtb infection and perhaps shorten the treatment regimen in patients.

Herein, we utilized the peptide DAB-10, composed of an Amino Terminal Copper and Nickel (ATCUN) binding motif and a C-terminal domain from a cell-penetrating antimicrobial peptide (AMP) as an anti-mycobacterial agent. The Cu-ATCUN complex produces ROS under physiologically relevant conditions.[23] Furthermore, recent studies have shown that ticks and fish express ATCUN-containing AMPs having a Cu-dependent mechanism of action.[24, 25] By coupling this copper-chelating moiety to a cell-permeable peptide, we aimed to develop a conjugate that could potentially bind intracellular Cu (to which Mtb is normally resistant) and harness the chemical reactivity of the resulting metallopeptide to generate endogenous ROS (to which Mtb is susceptible). We demonstrate here that DAB-10 requires Cu ions to kill mycobacteria via an oxidative stress mechanism and present the first unambiguous evidence that phagosomal Cu plays a critical role in eliminating intracellular Mtb.

RESULTS

Design Principles and Antimycobacterial Activity of DAB-10.

Our previous work on the ATCUN motif included the generation of D-ATCUN-D-*sh*-Buforin-10 (DAB-10), an all-D amino acid peptide with the sequence $_{D}$VIHRAGLQFPVGRVHRLLRK-NH_2.[26] The ATCUN binding motif, Val-Ile-His (selected due to its high ROS forming activity[27]) was coupled to residues 5 through 21 of the AMP Buforin II. Derived from Histone H2A, Buforin II binds isolated DNA and is hypothesized to inhibit bacterial growth also through DNA binding.[28] Converting L- to D-amino acids served to increase oxidative turnover of the ATCUN motif[23] and to confer protease resistance to DAB-10. We have previously shown that DAB-10 can oxidatively cleave DNA *in vitro* and in living *Escherichia coli* cells.[26] We hypothesized that DAB-10 would have anti-mycobacterial activity and that host-derived Cu ions would mediate activation. As an internal control, we utilized DAB-6 ($_{D}$RAGLQFPVGRVHRLLRK-NH_2), a peptide identical to DAB-10 which lacks the ATCUN motif (and by extension, lacks direct oxidative capabilities), to determine the relevance of Cu-binding to the mechanism of DAB-10.

We started by measuring the minimum inhibitory concentration (MIC) of both peptides against several *Mycobacterium* strains, including MDR and XDR patient isolates of Mtb (BND320, Jal2287, and Myc431) in a standard broth microdilution assay. We found that DAB-10 was more active than DAB-6 (to varying degrees) against several strains (Table 1). It should be noted that both DAB-6 and DAB-10 had activity against all mycobacterial strains tested (as well as other bacteria[26]), suggesting that these peptides likely do not bind a specific protein but rather invoke a more generalized toxicity. The increased potency observed in DAB-10 is consistent with a gain-of-function phenotype afforded by ATCUN motif conjugation. However, the conservative decrease in MIC is likely due to the possibility that DAB-10 is not Cu-saturated as it competes with bovine serum albumin (BSA) for limited amounts of the metal. BSA is present in the growth medium and also has an ATCUN motif.

Table 1. Minimum Inhibitory Concentration of the Peptides.

Mycobacterial Species	Minimum Inhibitory Concentration (MIC), μM	
	DAB-6	**DAB-10**
M. tuberculosis H37Rv	8	2
M. tuberculosis BND320[a]	8	4
M. tuberculosis Jal2287[a,b,c]	16	4
M. tuberculosis Myc431[a,b,c,d]	8	4
M. smegmatis mc^2155	0.5	0.125
M. bovis BCG (SSI 1331)	4 – 8	0.5 – 1

[a]Strain resistant to isoniazid, [b]Strain resistant to streptomycin, [c]Strain resistant to rifampicin, [d]Strain resistant to ethionamide.

DAB-10 Promotes Cu-Dependent Oxidative Stress Which Contributes to its Potency.

To determine the Cu-dependence of DAB-10 activity, we performed kill-kinetics studies against Mtb under copper-replete and -deplete conditions. We added either 50 μM of $CuCl_2$ or 100 μM of tetrathiomolybdate (TTM), a Cu-selective, cell-permeable chelator[29] to the growth medium prior to DAB-10 treatment. We found that varying the levels of available Cu did not affect either DAB-6 or isoniazid (INH) activity; however, DAB-10 was significantly more bactericidal in the presence of excess Cu (Figure 1A-1C). We emphasize that, in the presence of Cu, a greater bactericidal activity was observed for DAB-10 relative to DAB-6 despite the use of a four-fold lower dose (MIC DAB-6 = 4X MIC DAB-10), indicating that while the ATCUN motif only decreases the MIC up to four-fold, it increases the kill rate, which is of utmost importance in shortening drug treatment for TB patients. Additionally, we observed a similar phenotype for *M. smegmatis* (Msm) treated with DAB-10 at its MIC (Figure S1A), indicating similar Cu-dependent mycobacterial susceptibility to DAB-10.

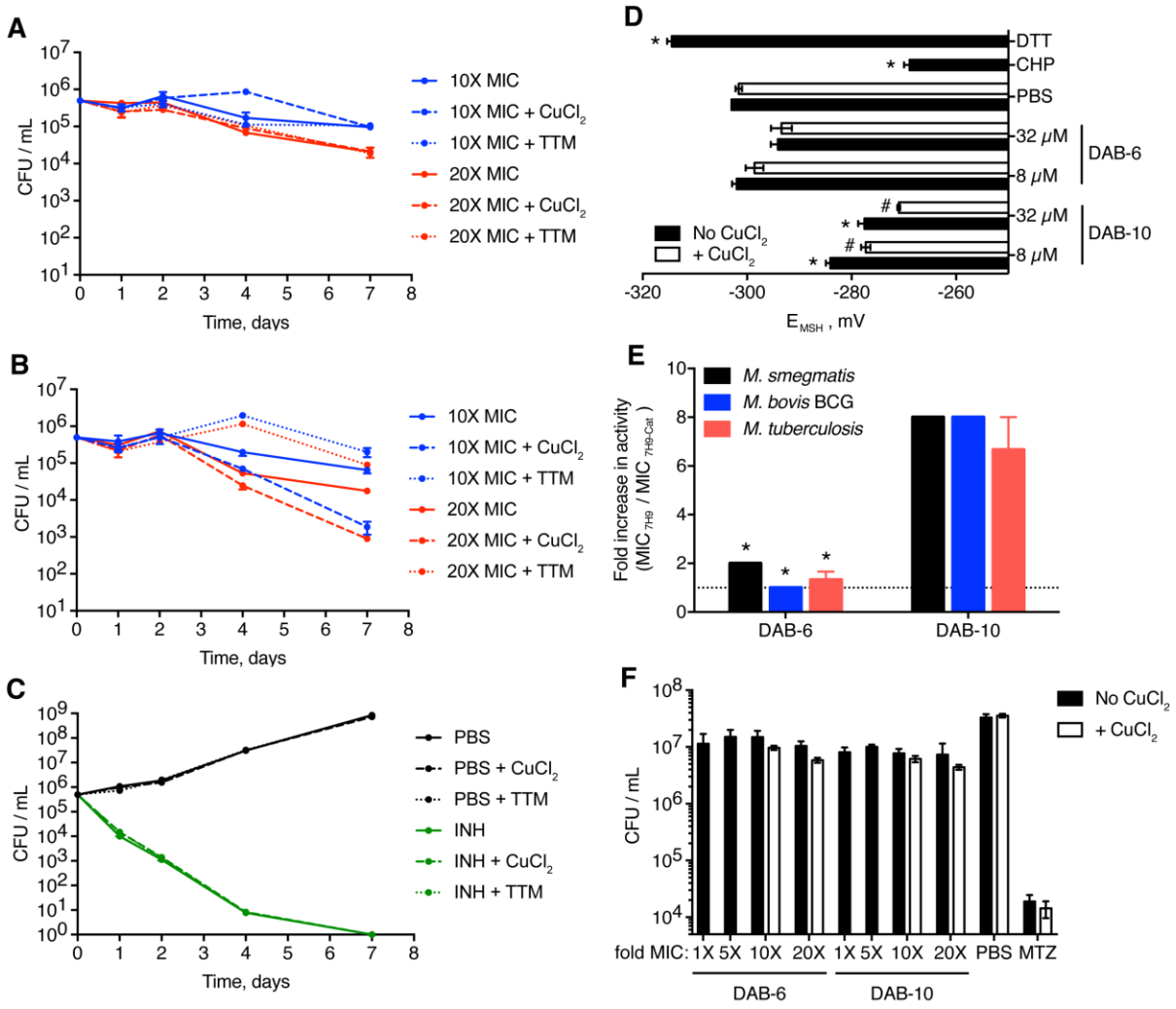

Figure 1. Cu-Dependent Oxidative Activity of DAB-10. (A-C) Time-Kill curves of Mtb cells treated with (A) DAB-6, (B) DAB-10 and (C) INH with either 50 μM $CuCl_2$ or 100 μM TTM. Data represent mean ± SEM (n = 2 triplicates) (D) Ratiometric fluorescence of Mrx1-roGFP2-expressing Mtb was converted to E_{MSH} values following treatment with either DAB-6 or DAB-10 (with and without 50 μM $CuCl_2$) at the indicated concentration, 40 mM of DTT, or 1 mM CHP. *, $P<0.01$ compared to buffer (PBS) control and #, $P<0.05$ compared to absence of $CuCl_2$. Bars represent mean ± SEM (n = 3 duplicates) (E) MIC of the compounds were measured in either complete media (7H9) or media without catalase (7H9-Cat) for three different mycobacterial species. Bars represent mean ± SEM (n = 3 duplicates) of ratio of MIC values with and without the enzyme. *, $P<0.01$ compared to corresponding DAB-10 treatment. (F) Activity of the compounds against non-replicating Mtb H37Rv in hypoxic conditions with or without 50 μM $CuCl_2$ using 100 μM metronidazole (MTZ) as a positive control. Bars represent mean ± SEM (n = 2 duplicates).

Following confirmation of the Cu-dependence in the activity of DAB-10, we set out to determine

whether this peptide induces oxidative stress. For this purpose, we employed the genetically encoded, ratiometric, fluorescent probe Mrx1-roGFP2,[30] a fusion of mycoredoxin-1 and redox-sensitive GFP, to report on the redox state of DAB-10-treated mycobacteria (Figure S1B). The Mrx1-roGFP2 biosensor measures the redox potential (E_{MSH}) of the most abundant cytoplasmic antioxidant of mycobacteria, mycothiol (MSH).[30] We first generated a calibration curve using Mrx1-roGFP2-expressing Msm and Mtb treated with various ratios of the oxidized and reduced forms of dithiothreitol (DTT, 10 mM total) corresponding to known E_{MSH} values based on the Nernst Equation (Figure S1C and S1D) as previously described.[30] Treatment of Mtb with DAB-6 resulted in modest shifts in E_{MSH} values, while DAB-10 treatment resulted in significant dose- and Cu-dependent perturbation in E_{MSH}. Using DTT as reductant and cumene hydroperoxide (CHP) as oxidant controls, we confirmed that a shift towards more positive E_{MSH} values implies that cells experience oxidative stress upon exposure to DAB-10, but not during DAB-6 treatment (Figure 1D). A similar phenotype was observed with DAB-10-treated Msm (Figure S1E and S1F), although E_{MSH} values were markedly more positive ($P<0.05$) compared to those in Mtb, indicating that Msm experienced greater oxidative stress. The trend in E_{MSH} between DAB-10-treated Msm and Mtb remarkably traced the trend in MICs, indicating that the potency of DAB-10 against these two species is highly correlated to the extent of oxidative stress it induces.

As a supplementary measure of oxidative stress, we employed the TUNEL assay to measure oxidative DNA damage. We observed a two- to three-fold increase in TUNEL-positive cells upon DAB-10 treatment which decreased upon addition of TTM (Figure S1G) further signifying that intracellular oxidation of DAB-10 resulted from Cu binding.

To further demonstrate that the oxidative activity of DAB-10 determines its mycobactericidal effect, we tested the survival of mycobacteria in growth medium (7H9) with or without catalase. Removal of catalase did not affect the potency of DAB-6 in any of the *Mycobacterium* species tested. On the other hand, DAB-10 activity increased six- to eight-fold upon removal of the enzyme (Figure 1E), indicating that in the absence of an H_2O_2 scavenging system, DAB-10 activity was potentiated. Because catalase affects the potency of DAB-10 without gaining access to the mycobacterial cytosol, our results suggest that H_2O_2

generated extracellularly plays a role in mycobacterial killing by DAB-10. H_2O_2 is stable and diffusible enough to pass through both the outer and inner membrane of bacteria such as *E. coli* and *Salmonella*.[31, 32] Our interpretation is that cytoplasmic metallated DAB-10 can react with H_2O_2 molecules that diffuse into *Mycobacteria* to produce potent reactive oxygen species.

Finally, we tested the activity of our compounds against Mtb that were rendered non-replicating by gradual depletion of oxygen. Three-week old cultures grown in air-tight flasks were treated with DAB-6 or DAB-10 inside an anaerobic chamber for 7 days and spread on 7H11 plates for colony enumeration. We found that across all concentrations tested, the activity of DAB-10 and DAB-6 were equal, with both compounds causing similar modest inhibition (Figure 1F). Thus, a certain oxygen tension is required by DAB-10 for it to become more active than DAB-6. No Cu dependence was observed in DAB-10 activity against non-replicating Mtb consistent with the fact that ROS cannot be formed without oxygen regardless of how much of the metal co-factor is present.

Taken altogether, the results from multiple independent procedures converge to support the conclusion that DAB-10 induces Cu-dependent oxidative stress *in vitro* which likely plays a major role in its bactericidal mechanism.

DAB-10 and Mycobacteria Rendezvous Inside Macrophages.

Because access to the mycobacteria-containing phagosome is required for efficient Mtb eradication, we next tested whether DAB-10 can reach regions containing intracellular mycobacteria. We first incubated RAW264.7 macrophages with 4 μM of a tetramethylrhodamine (TMR)-labeled version of DAB-10 (the fluorophore was attached to the N-terminal of the peptide). We observed distinct punctate localization reminiscent of cytosolic vesicles (Figure 2A), indicating a possible mode of internalization involving endocytosis. This localization was observed for DAB-10 even at concentrations as low as 1 μM and was observed for DAB-6 (Figure S2A), indicating that cell uptake is not dictated by the ATCUN motif. When we co-treated macrophages with 50 μM amiloride, a compound that inhibits macropinocytosis by lowering submembranous pH and inhibiting Rac1 and Cdc42 activation,[33] we observed DAB-10

localization similar to that of the untreated cells (Figure S2B). However, in the presence of 80 μM dynasore which inhibits dynamin-mediated endocytosis, DAB-10 localized in the mitochondria. This observation suggests that while DAB-10 can translocate across biological membranes, it is preferably internalized by macrophages via clathrin-coated vesicles.

We then infected RAW264.7 cells with Msm (Multiplicity of Infection, MOI 1:100) or Mtb (MOI 1:10) prior to incubation with 4 μM of DAB-10-TMR. We found that DAB-10 encountered both intracellular mycobacteria as early as 30 mins post-exposure (Figure 2B-2E) as determined by the Costes P-value (Mean P-value = 0.98 from 28 Mtb-infected macrophages). The images also show that intracellular mycobacteria were homogeneously stained by DAB-10. Indeed, treatment of Msm (grown in axenic cultures) with DAB-10-TMR resulted in the same phenotype (Figure S2C), suggesting that DAB-10 can traverse the mycobacterial membrane. Additionally, we were able to observe DAB-10 accumulating outside the cytoplasmic space (due to the low resolution we were unable to determine whether the peptide accumulates in the membrane or the periplasmic space. Alternatively, DAB-10 could be localized in the capsule layer or bound to the cell wall peptidoglycan/arabinogalactan layer, Figure S2D and S2E) of intracellular Mtb, an intermediate step ultimately leading to the intrabacterial localization of DAB-10.

We assume that the DAB-10-containing and mycobacteria-containing phagosomes fuse at the stage of early to late endosomes because neither the bacteria nor the peptide co-localize with lysosomes after 30 min (Figure S2F). Only after 3 hrs were the lysosomes found to fuse with Msm-containing phagosomes. Finally DAB-10 co-localization with intracellular mycobacteria is a function of the peptide being routed through the endocytic pathway, as addition of dynasore abolished peptide and mycobacteria co-localization (Figure S2F). Overall, our data demonstrate that DAB-10 can physically target intracellular mycobacteria.

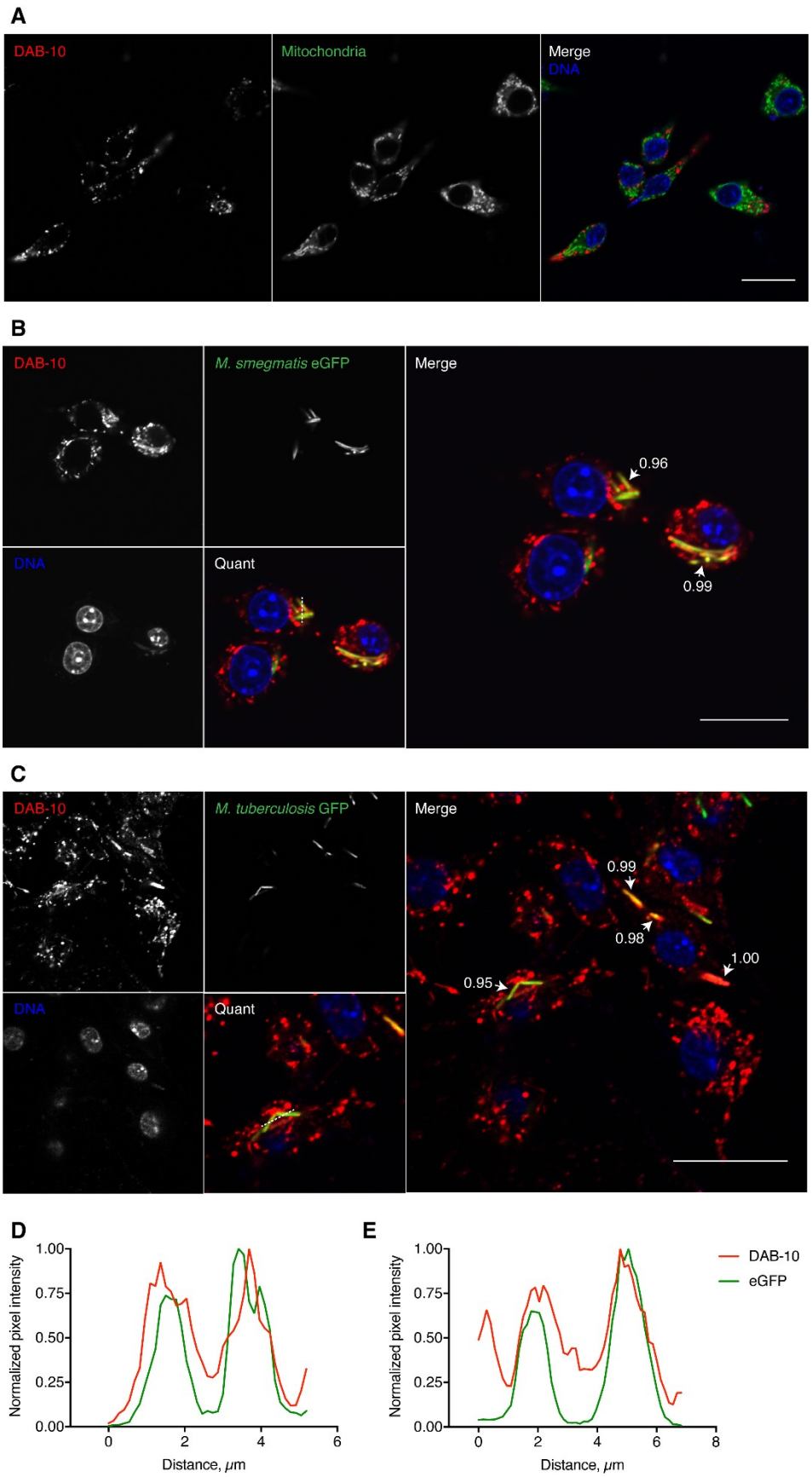
A
DAB-10
Mitochondria
Merge
DNA
B
DAB-10
M. smegmatis eGFP
Merge
0.96
0.99
DNA
Quant
C
DAB-10
M. tuberculosis GFP
Merge
0.99
0.98
1.00
0.95
DNA
Quant
D
Normalized pixel intensity
1.00
0.75
0.50
0.25
0.00
0
2
4
6
Distance, μm
E
Normalized pixel intensity
1.00
0.75
0.50
0.25
0.00
0
2
4
6
8
Distance, μm
DAB-10
eGFP

Figure 2. Intracellular Localization of DAB-10. (A) RAW264.7 cells were incubated with tetramethylrhodamine (TMR)-labeled DAB-10 and its localization was followed by laser confocal microscopy. (B and C) GFP-expressing Msm (B) and Mtb (C) were used to infect RAW264.7 cells prior to incubation with DAB-10-TMR. Merge channels show the Costes P-value of colocalization in the bacteria pointed by the white arrows. Scale bars = 20 μm. (D and E) The pixel intensity along the dashed line in Msm- (D) and Mtb-infected (E) macrophages in the Quant channel was plotted against length of the line to show encounter between DAB-10 and mycobacteria.

DAB-10 Binds to Phagosomal Copper.

We next sought to determine whether DAB-10 can competitively sequester Cu in the intracellular milieu. We first synthesized CS-1 (Figure S3A), a Cu-selective fluorescent probe[34] to determine whether DAB-10 co-localizes with the metal. Incubation of RAW264.7 cells with fluorescein-labeled DAB-10, (DAB-10-FL) and CS-1 showed fluorescence co-localization within distinct puncta (Costes P-value 0.88-0.95, Figure S3B). Co-localization improved when macrophages were activated with LPS (Costes P-value 0.97-0.98). This indicates that DAB-10 and Cu are in close proximity, making metal binding possible.

We next examined whether direct metal binding occurs within macrophages. For this purpose, we exploited the fluorescence quenching properties of Cu[34] and designed DAB-10 derivatives that differed in the position of the fluorophore with respect to the ATCUN motif. We attached TMR (a pH insensitive fluorophore) to the ε-amino group of either Lys-20 [DAB-10-K_{20}(TMR)] or an extra Lys placed immediately after the ATCUN motif [DAB-10-K_4(TMR)], and reasoned that since TMR is closer to the metal in the K_4 derivative, DAB-10-K_4(TMR) should exhibit fluorescence quenching upon Cu binding. Not surprisingly, we observed a ~35% decrease in emission intensity *in vitro* when 1 equivalent of Cu was added to DAB-10-K_4(TMR) but not when the same amount of Cu was added to DAB-10-K_{20}(TMR) (Figure S4A). Confocal microscopy using constant instrument settings revealed that DAB-10-K_4(TMR) exhibited minimal fluorescence (irrespective of LPS addition) which was later rescued upon addition of the competitive Cu chelator, TTM (Figure 3A and 3B). On the other hand, strong intracellular fluorescence

was observed for DAB-10-K_{20}(TMR) with a similar intensity upon macrophage activation. To ensure that the differences in fluorescence intensity were not a result of decreased peptide uptake, we quantified the intracellular concentration of both DAB-10 derivatives (Figure 3C). We found that at 4 μM, the concentration at which the microscopy experiments were done, both DAB-10-K_4(TMR) and DAB-10-K_{20}(TMR) were taken up by RAW264.7 cells to similar extents (~0.1 nmol/mg of protein). Thus, the weaker fluorescence intensity by DAB-10-K_4(TMR) is not an experimental artifact, but rather a result of direct Cu binding within the cell. We note that a similar fluorescence intensity and cell uptake profile were observed for the same set of DAB-10 derivatives labeled with fluorescein (Figure S4B-S4E), indicating that the observed phenotype is independent of the identity of the fluorophore.

Finally, using Isothermal Titration Calorimetry (ITC), we found that DAB-10 binds to Cu^{2+} with a sub-micromolar affinity (calculated apparent K_d = 547 ± 123 nM, Figure 3D) under pH 6.40, simulating arrested acidification of the Mtb-containing phagosome.[35] Together with the fact that following infection with Mtb, intraphagosomal Cu reaches concentrations an order of magnitude above the observed K_d,[9] our data thus far indicated that DAB-10 is likely Cu-bound inside Mtb-infected macrophages. Retrospectively, a submicromolar dissociation constant might explain why we observed a dramatic enhancement in bactericidal activity when copper was exogenously added during the kill-kinetic studies of DAB-10 (Figure 1B). BSA (which also binds Cu through an ATCUN motif) in the media likely competes with DAB-10 for any traces of Cu present in 7H9 medium.[11]

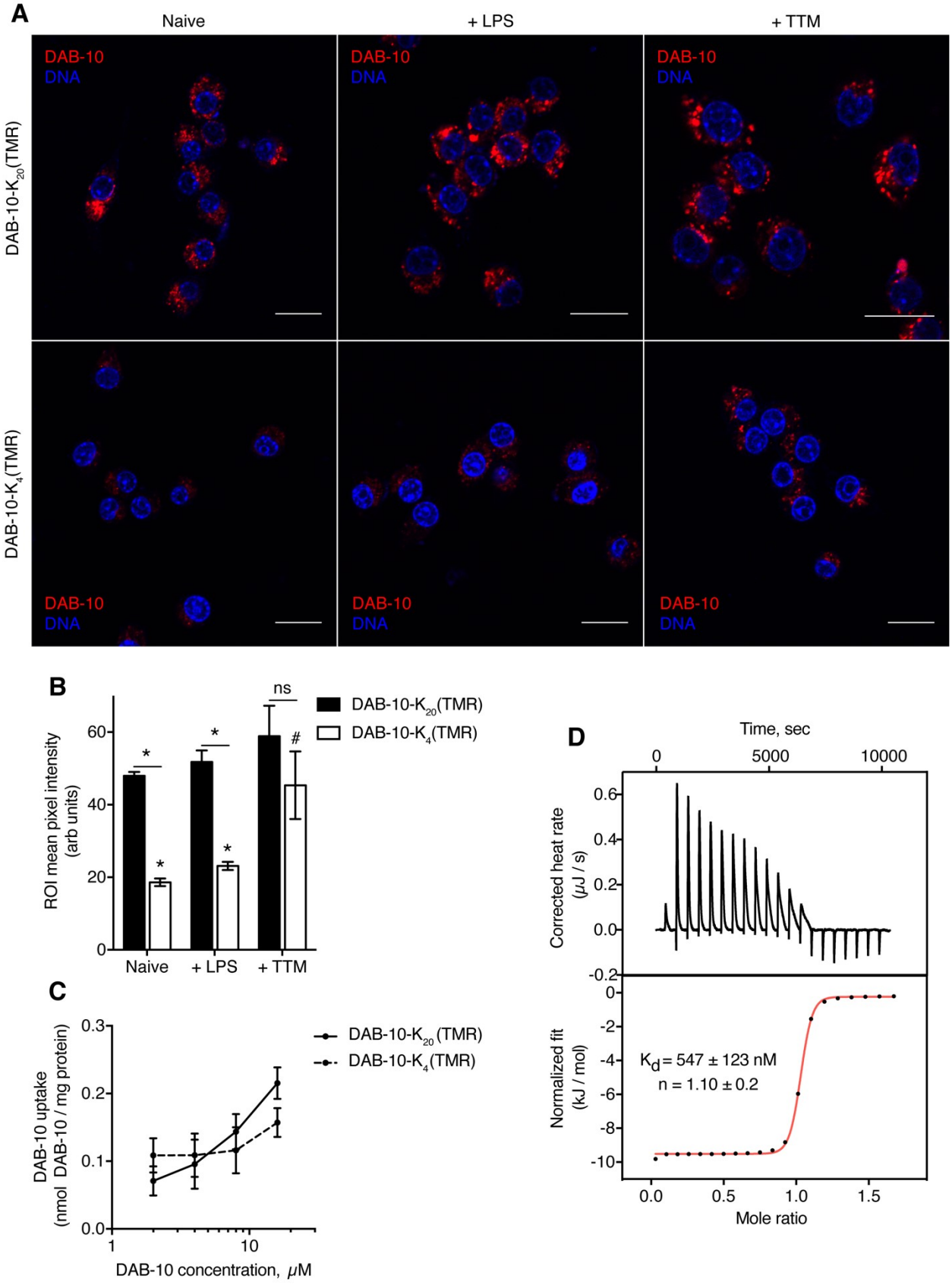
A
Naive
+ LPS
+ TTM
DAB-10-K20(TMR)
DAB-10-K4(TMR)
DAB-10
DNA
B
ns
DAB-10-K20(TMR)
DAB-10-K4(TMR)
ROI mean pixel intensity (arb units)
Naive
+ LPS
+ TTM
C
DAB-10-K20(TMR)
DAB-10-K4(TMR)
DAB-10 uptake (nmol DAB-10 / mg protein)
DAB-10 concentration, μM
D
Time, sec
Corrected heat rate (μJ / s)
Normalized fit (kJ / mol)
Kd = 547 ± 123 nM
n = 1.10 ± 0.2
Mole ratio

Figure 3. Intracellular Cu Binding of DAB-10. (A) 4 μM of DAB-10 derivatives differing in the position of the TMR label were added to naïve or activated RAW264.7 in the presence or absence of TTM. Images were acquired using the same instrument setting and scale bars = 20 μm. (B) Regions of interests (ROIs) were drawn in the red channel to cover the entire fluorescent portion of each cell. Pixel intensities were then obtained from FIJI (Image J) analysis. Bars represent mean ± SEM (n ≥ 5 cells) (C) RAW264.7 cells were incubated with varying amounts of the K_{20}(TMR) or the K_4(TMR) derivative for 1 hr followed by fluorescence quantification of the cell lysate. Data represent mean ± SD (n = 3 duplicates) (D) Isothermal Titration Calorimetry (ITC) was used to determine binding constant of DAB-10 to Cu(II) at pH 6.40. Data shown are representative of three independent trials.

Phagosomal Copper is Necessary for Oxidative Attack on Intracellular *M. tuberculosis*.

Having confirmed Cu-dependent oxidative activity and intracellular Cu scavenging of DAB-10, we proceeded to determine whether it uses the metal for its activity against intracellular Mtb. We first examined the toxicity of DAB-10 in naïve macrophages using a standard viability assay. We found that DAB-10 at concentrations up to 256 μM has negligible toxicity against THP-1 (Figure 4A) and RAW264.7 (Figure S5A) cells, consistent with the negligible toxicity of DAB-10 against epithelial and HEK293 cells that we had previously observed.[26]

We next infected differentiated THP-1 cells with *M. tuberculosis* H37Rv (MOI 1:5) in DMEM spiked with 5 μM of $CuCl_2$ and measured bacterial survival following peptide treatment. We observed early bactericidal activity for both peptides at 10X their *in vitro* MIC (80 μM for DAB-6 and 20 μM for DAB-10) 48 hrs after exposure to the peptide (Figure S5B) and a dose-dependent mycobacterial killing at the 4th and 7th day of treatment (Figure 4B and 4C). To unambiguously determine whether phagosomal Cu is involved, we co-treated infected macrophages with the peptides and an excess of either TTM (cell-permeable) or BCS (bathocuproinedisulfonate, cell-impermeable).[7, 36] We hypothesized that by using Cu-specific chelators with various permeability profiles, we could determine, without bias, whether

intracellular or extracellular Cu is utilized by DAB-10. For both time points (day 4 and 7), DAB-6 activity was unaffected by the presence of the chelators, indicating that it does not utilize Cu for its activity (Figure 4B and 4C). However, we observed a significant decrease in DAB-10 activity only in the presence of TTM. This difference was particularly pronounced at day 7 of treatment (Figure 4C). Since only the cell-permeable chelator attenuated the activity of DAB-10, our data indicates that intracellular, rather than extracellular Cu is involved in DAB-10 activity. Moreover, because DAB-10 is restricted within endosomes (Figure 2A), our results also demonstrate that phagosomal Cu (not the cytosolic Cu) is utilized by DAB-10. It should be noted that neither the buffer (PBS) nor the positive (INH) control showed Cu-dependence. Furthermore, at 100 μM of the chelators, THP-1 viability was unaffected (Figure S5C). Overall, our results demonstrate that DAB-10 utilizes phagosomal Cu to kill intracellular *M. tuberculosis*.

We next determined whether intracellular Mtb experiences oxidative stress during DAB-10 treatment. For this purpose, we infected differentiated THP-1 cells with Mtb expressing the redox sensor Mrx1-roGFP2 (MOI 1:10) and treated the cells for 24 hrs prior to fluorescence measurement. We found that intracellular Mtb treated with DAB-10 showed more positive E_{MSH} relative to those treated with DAB-6 (Figure 4D), consistent with a more oxidative environment. We recorded a significant oxidative shift in INH-treated cells as well, in accordance to previously reported oxidative shifts induced by several anti-TB drugs.[30] More importantly, DAB-10 effects are distinct from those of INH because we observed a shift towards less oxidizing E_{MSH} values upon addition of TTM. This indicates that while the oxidative stress experienced by intracellular Mtb treated with INH is largely a result of downstream induction of ROS (a consequence of the drug's bactericidal effect), a significant fraction of the oxidative stress in DAB-10-treated Mtb is a result of Cu-promoted ROS formation.

Finally, due to the desirable activity of DAB-10 in an *ex vivo* model of infection, we wanted to determine its efficacy *in vivo* using an acute TB model of infection. BALB/c mice were aerosol infected with Mtb H37Rv and treated with 5 mg/kg of either DAB-6 or DAB-10. The treated and untreated mice were further divided into two groups, one fed with pure water and the other fed with water containing 118 mg/L of $CuSO_4$ – a concentration previously shown to have no adverse effects on mice.[11] With and without

copper supplementation, DAB-6 exhibited surprising acute toxicity as all mice became moribund shortly after initiation of treatment. Mice in the DAB-10 treatment group exhibited no significant adverse effects. After 7 days, mice in the DAB-10 and control treatment groups were sacrificed. We found no significant difference in bacterial burden between mock-treated mice and DAB-10-treated mice (Figure S5D). Furthermore, $CuSO_4$ in the drinking water did not potentiate the activity of DAB-10. We suspect that the dismal *in vivo* efficacy of DAB-10 can be attributed to serum albumin binding as both DAB-6 and DAB-10 exhibited a 32-fold higher activity against Mtb in growth medium containing casitone in place of BSA (DAB-6 MIC = 0.5μM and DAB-10 MIC = 0.06 μM). Not surprisingly, albumin binding has been shown to significantly lower the activity of cationic antimicrobial peptides.[37, 38] Because albumin binding by AMPs is largely a result of physicochemical interactions,[39] fine-tuning the sequence, length and lipophilicity of DAB-10 might increase its serum bioavailability and consequently increase its antimycobacterial activity. Indeed, in a study of tripeptides, greater lipophilic character largely resulted in higher albumin binding.[37] Additionally, peptides with a higher zeta potential were found to have a greater efficacy *in vivo* likely due to diminished protein binding.[40] Notwithstanding sequestration by albumin, the therapeutic potential of DAB-10 is evident when examining its synergy with current anti-TB drugs. We observed synergistic interactions between DAB-10 and rifampicin (fractional inhibitory concentration, FIC indices = 0.38-0.50, Figure S5E) against both Mtb and *M. bovis* BCG. Similar synergistic interactions of rifampicin with ROS and ROS-forming compounds have been reported[41-43] and have predominantly been attributed to increased rifampicin uptake or an additive hydroxyl radical induction by both compounds. However, we speculate that DAB-10-promoted oxidative DNA damage can exacerbate the action of rifampicin – which sterically occludes RNA polymerase (RNAP), preventing elongation[44] – either by stalling RNAP or promoting its dissociation at the DNA lesion sites.

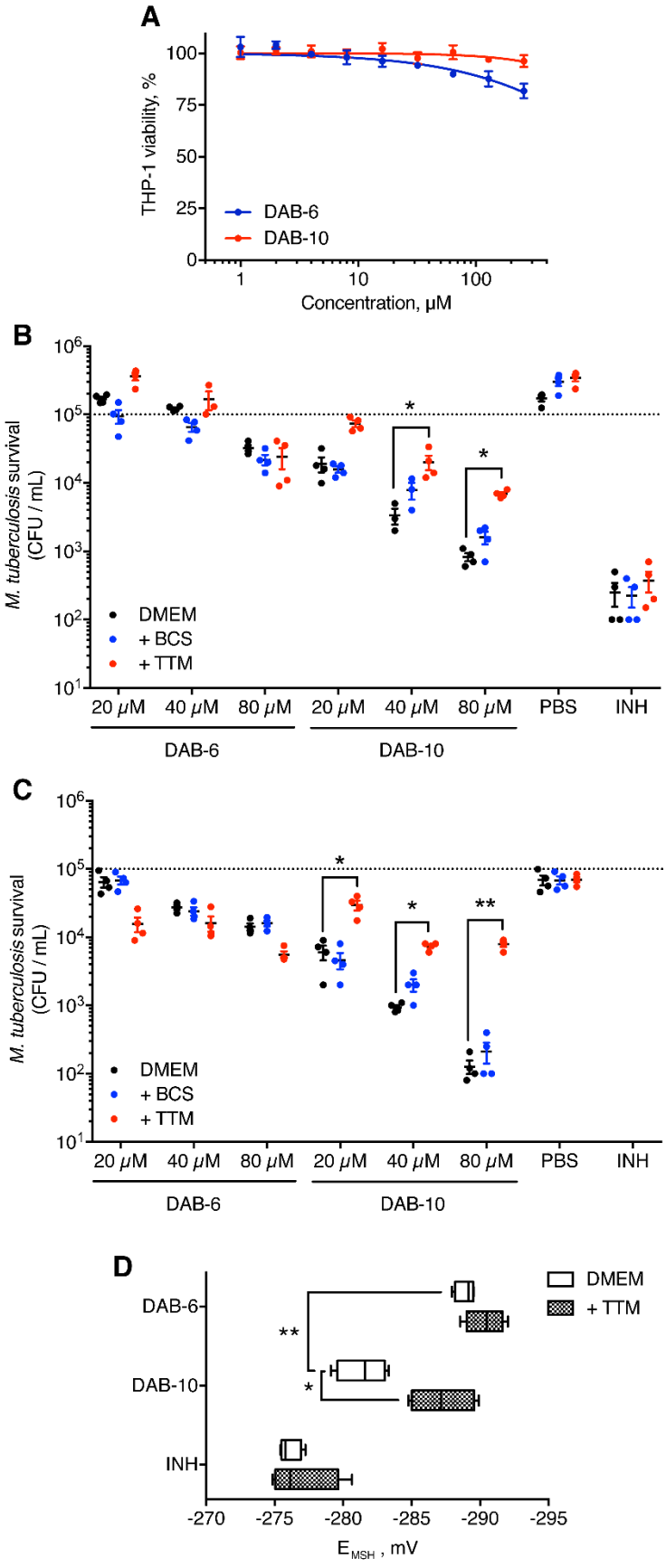
A
THP-1 viability, %
100
75
50
25
0
DAB-6
DAB-10
1
10
100
Concentration, μM
B
M. tuberculosis survival (CFU / mL)
10^6
10^5
10^4
10^3
10^2
10^1
DMEM
+ BCS
+ TTM
*
*
20 μM
40 μM
80 μM
20 μM
40 μM
80 μM
PBS
INH
DAB-6
DAB-10
C
M. tuberculosis survival (CFU / mL)
10^6
10^5
10^4
10^3
10^2
10^1
DMEM
+ BCS
+ TTM
*
*
**
20 μM
40 μM
80 μM
20 μM
40 μM
80 μM
PBS
INH
DAB-6
DAB-10
D
DAB-6
DAB-10
INH
**
*
DMEM
+ TTM
-270
-275
-280
-285
-290
-295
E_{MSH}, mV

Figure 4. Cu-dependent Oxidative Activity of DAB-10 Against Intracellular *M. tuberculosis*. (A) Cytotoxicity of synthesized peptides against THP-1 cells was assessed by the MTT assay after 48 hrs. Data represents Mean ± SEM (n = 3 duplicates) (B and C) Differentiated THP-1 cells were infected with Mtb H37Rv (MOI 1:5) prior to incubation with peptides at the indicated concentration in the presence or absence of 100 μM of the copper chelators (TTM or BCS). Survival of Mtb was measured after 4 days (B) and 7 days (C) by plating dilutions in 7H11. Data represents mean ± SEM (n = 2 duplicates). *, $P<0.05$; **, $P<0.01$. Dotted line represents starting Mtb inoculum. INH (5 μM) after 7 days had bacterial counts that fell below the limit of detection of the assay (~10 CFU/mL). (D) THP-1 cells infected with Mtb expressing the redox sensor Mrx1-roGFP2 were treated with peptides at 40 μM or 5 μM of INH for 12 hours and fluorescence was read using a plate reader. Boxes represent mean ± SEM (n = 2 duplicates). *, $P<0.05$; **, $P<0.01$.

DISCUSSION

The influx of Cu ions into the mycobacterial phagosome, resulting from the concerted action of Cu transporters (Ctr1 and ATP7A) and chaperones (Atox1),[45] represents an untapped resource for novel therapeutic interventions. Agents that harness this exchangeable metal pool would circumvent the Cu resistance of Mtb[8] without requiring secondary exogenous factors. Furthermore, because Cu tends to accumulate during infection,[46] it has been suggested that compounds that turn into potent antimicrobials in the presence of Cu can be used to control bacterial growth *in situ*.[15] The promise of this approach has been tested using small organic molecules that acquire anti-mycobacterial activity upon binding to Cu[14-16]. However, these studies lacked explicit evidence for a direct phagosomal Cu involvement. Herein, we present explicit evidence of a peptide phagosomal Cu for its anti-mycobacterial activity. Our approach combines the exploitation of host-derived Cu ions with susceptibility of Mtb to ROS, to generate an activatable oxidant for the inhibition of intracellular Mtb.

The observation that DAB-10, but not DAB-6, exhibits Cu-dependent redox cycling supports the notion that the addition of the ATCUN motif results in a gain-of-function phenotype that affords DAB-10 a secondary mode of attack. Indeed, DAB-6 displays a weaker potency relative to DAB-10, which we think stems from its ability to bind DNA, possibly resulting in inhibition of nucleic acid metabolism.[28] Conversely, we propose that a major contributor to the activity of DAB-10 is its redox cycling. However, we cannot completely exclude the possibility that DAB-10 also inhibits growth in a manner similar to DAB-6, especially since both peptides exhibited similar residual activity against Mtb rendered non-replicating by hypoxia. Our data certainly support a mechanism that involves a target present in both replicating and non-replicating Mtb (such as genomic DNA) or a toxic agent able to damage both states of Mtb (such as ROS). We conclude that not only can DAB-10 overwhelm the bacteria with ROS, but it can also elicit an inhibitory effect independent of its oxidative ability, a route it can take when surrounding Cu levels are not sufficient for binding.

While it has been consistently shown that bactericidal antibiotics induce the formation of deleterious hydroxyl radicals by liberating ferrous ions (from iron-sulfur clusters) that promote the Fenton reaction,[47, 48] evidence that argue against this model also exist[49, 50]. The observation of a Cu-dependent oxidative stress experienced by DAB-10-treated cells suggests that instead of inducing the formation of ROS, metallated DAB-10 is directly producing ROS. While the exact mechanism of ROS formation by Cu-ATCUN complexes is still a matter of debate,[51] the accepted pathway proposed by Cowan and co-workers[23] involves the initial formation of a peroxo-bridged Cu-ATCUN dimer that then forms a hydroperoxide anion (technically a deprotonated H_2O_2). This hydroperoxide anion is then involved in the reduction of another Cu-ATCUN complex to form a Cu-bound hydroxyl radical, the actual ROS in this context (Eqns 1-3). From this scheme, it can easily be seen why catalase attenuates DAB-10 activity, because in the presence of the H_2O_2 scavenging enzyme, reaction 3 cannot occur, terminating the reaction series prior to formation of the active oxidant.

$$2\ LCu^{II} + O_2 + 2\ e^- \dashrightarrow LCu^{II}\text{-}O\text{-}O\text{-}Cu^{II}\text{-}L \quad (1)$$

$$LCu^{II}\text{-}O\text{-}O\text{-}Cu^{II}\text{-}L + H^+ \dashrightarrow 2\ LCu^{II} + \mathbf{HO_2^-} \quad (2)$$

$$LCu^{II} + \mathbf{HO_2^-} + e^- + H^+ \dashrightarrow LCu^{II}\text{-}OH + OH^- \quad (3)$$

Central to our strategy is the ATCUN motif, which performs both Cu-binding and oxidative chemistry in DAB-10. While most of the Cu in Middlebrook 7H9 (~6.3 μM) is sequestered by albumin (which also contains an ATCUN motif), we presumed that not adding exogenous Cu simulates conditions of metal competition that are relevant physiologically. We assume that DAB-10 is metallated upon exposure to 7H9 because its K_d is significantly lower than the total Cu content of the growth medium. The binding constants to Cu(II) previously measured for the ATCUN motif of Ctr1[52] are close to those of Human Serum Albumin (HSA)[53] indicating that competition for the metal between ATCUN motifs of various sequences may occur and, if it does, is bidirectional. Depletion of Cu in 7H9 via the addition of the high affinity chelator TTM attenuated DAB-10 potency, signifying Cu dependence of its activity. While DAB-10 in our experiments may not be saturated with Cu, the fact that the ROS formation by the Cu-ATCUN motif is catalytic[23] suggests that a small population of metallated DAB-10 can effect a similar, albeit weaker oxidative activity.

Because the oxidative activity of DAB-10 is a function of its Cu co-factor, the question of where DAB-10 acquires the metal becomes relevant. In the intracellular milieu, DAB-10 co-localized and bound directly to Cu regardless of whether resting or activated macrophages were used. The Cu(I) selective probe CS-1 used here was shown to have endosome-like localization (termed Cu "hotspots") in primary macrophages[54] similar to the distribution of DAB-10 in RAW264.7 macrophages. Taken together with the considerable affinity of the ATCUN motif toward Cu(I) as previously described for Ctr1[52], DAB-10 is most likely Cu-bound within resting macrophages. In addition, even though it is widely known that the reductive conditions in the cytoplasm favor Cu(I), the fact that endosomes are topologically equivalent to the extracellular environment[55] suggests that any Cu taken up during endocytosis is likely in the +2 state. These conditions generate a transient pool of Cu(II) which can serve as a metal source for DAB-10, making

formation of metallated DAB-10 probable. Finally, within macrophages infected with Mtb, it is even more plausible that DAB-10 is Cu-bound for the following reasons. First, naïve macrophages infected with *Mycobacterium avium*, or macrophages activated with IFN-γ prior to or following infection were shown to contain 17 μM, 82 μM, and 177 μM of Cu in the phagosome, respectively.[9] All of these reported concentrations are well above the measured K_d of Cu-DAB-10. Second, Mtb expresses a periplasmic multicopper oxidase (MmcO) that possibly converts Cu(I) to Cu(II).[13] Therefore, in the context of an infection, not only is there an abundant Cu supply in the phagosome, but this labile pool also contains Cu in the oxidation state preferred by DAB-10.

Combining our results, we propose a pathway through which DAB-10 oxidatively targets intracellular Mtb (Figure 5). Infected macrophages, regardless of activation, contain micromolar levels of Cu because of the transport pathways involving Ctr1, Atox1 and ATP7A. During DAB-10 treatment, the peptide is taken up via clathrin-mediated endocytosis and the resulting vesicle is uncoated in the cytosol. At this stage, a fraction of DAB-10 is probably already bound to Cu, but because of the depletion of reductive equivalence in a progressively maturing endosome, minimal redox cycling occurs. Intracellular Mtb acquires extracellular iron by gaining access to the transferrin recycling pathway,[9, 56] suggesting that the Mtb-containing phagosome can likely fuse with early endosomes. Therefore, bacteria and peptide co-localization occurs following fusion of the DAB-10-containing and Mtb-containing endosomes. Vesicular fusion affords DAB-10 access to high levels of Cu upon which metal sequestration ensues. DAB-10 likely translocates across the mycobacterial membrane in the metallated form; or if not, apo-DAB-10 can be metallated in the mycobacterial periplasm where Cu(II) is formed by MmcO. Finally, the biological reductants (i.e. MSH) present in the mycobacterial cytosol trigger the oxidative activity of DAB-10, resulting in Mtb death.

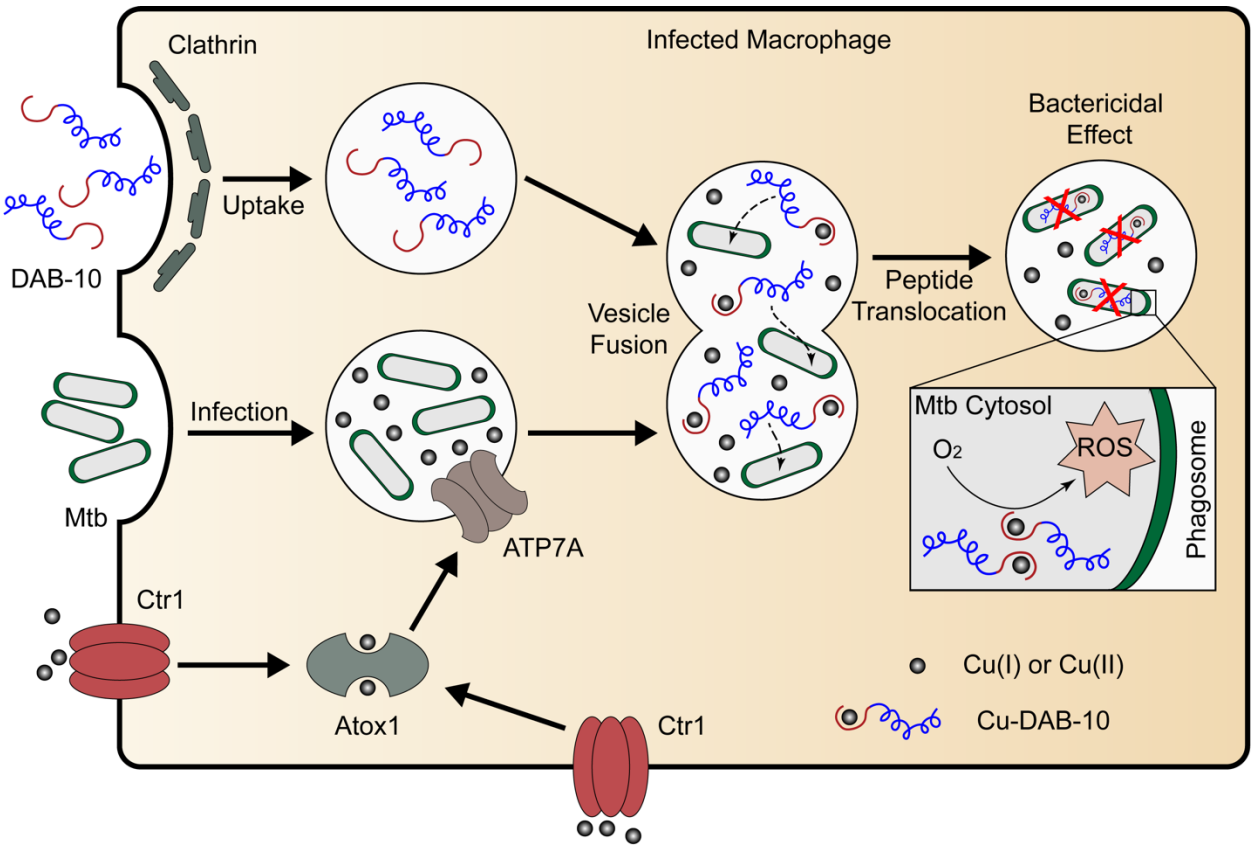

Figure 5. Proposed Mechanism of Action of DAB-10. Macrophages infected with Mtb take-up DAB-10 via clathrin-mediated endocytosis. DAB-10-containing vesicles fuse with the Mtb-containing phagosome allowing access to high levels of Cu. Binding of Cu triggers oxidative activity of DAB-10 against Mtb resulting in bacterial death.

In conclusion, our work describes a novel starting point from which to develop drugs that target both susceptible and drug-resistant Mtb for control of the devastating threat of TB. Compounds that can utilize various bioavailable resources within macrophages, especially the ones that are specifically upregulated during infection (including but not limited to transition metals) would augment the immunological response of phagocytes. Such compounds would also complement and diversify the current portfolio of anti-TB drugs. We build upon the proof-of-concept studies that exploit the profusion of Cu ions at the host-Mtb interface by using a system that not only binds Cu but also leverages the redox properties of Cu to generate ROS.

ASSOCIATED CONTENT

Supporting Information

Supplementary Materials and Methods describe the assays performed in these studies. Figures S1−S5.

ACKNOWLEDGEMENTS

The authors would like to thank Dr. Jorge L. Cervantes for the gift of eGFP-expressing *M. smegmatis* and Prof. Kenneth G. Campellone for the gift of THP-1 cells. C.F.-N. was supported by the Ramon Areces Foundation. The mouse infection work was made possible with help from the Harvard University Center for AIDS Research (CFAR), an NIH funded program (P30 AI060354). S.H.E.K. acknowledges support from EU FP7 project "ADITEC" (HEALTH-F4-2011-280873) and "PreDiCT-TB" (IMI JU Grant No. 115337). A.S. is a Senior Fellow of Wellcome Trust UK-DBT India Alliance. A.S. thanks the Department of Biotechnology (DBT), Ministry of Science and Technology, India BT/PR5020/MED/29/454/2012 and Wellcome-DBT India Alliance (500034/Z/09/Z) for financial support. A.M.A.-B. is supported by NSF (MCB-1715494), Lyme Disease Association and generous start-up funds from the University of Connecticut.

AUTHOR CONTRIBUTIONS

M.D.J.L., A.M.A.-B., A.S., S.H.E.K. conceptualized and designed the experiments. C.F.-N., S.C.P., and A.K.B. performed *in vivo* efficacy studies. G.K., and P.K. performed *ex vivo* efficacy studies, and K.A. measured MICs vs drug-resistant Mtb isolates. S.P. performed viability assays and C.D. and M.B.S. synthesized CS-1. M.D.J.L. performed all other experiments not specified above. M.D.J.L. wrote the manuscript with significant insights from C.F.-N., A.K.B., S.H.E.K., A.S., and A.M.A.-B.

REFERENCES

[1] World Health Organization (2017) Global tuberculosis report, Geneva.

[2] Sacchettini, J. C., Rubin, E. J., and Freundlich, J. S. (2008) Drugs versus bugs: in pursuit of the persistent predator Mycobacterium tuberculosis, *Nature reviews. Microbiology 6*, 41-52 DOI 10.1038/nrmicro1816.

[3] Kaufmann, S. H., Lange, C., Rao, M., Balaji, K. N., Lotze, M., Schito, M., Zumla, A. I., and Maeurer, M. (2014) Progress in tuberculosis vaccine development and host-directed therapies--a state of the art review, *Lancet Respir Med 2*, 301-320 DOI 10.1016/S2213-2600(14)70033-5.

[4] Neyrolles, O., Wolschendorf, F., Mitra, A., and Niederweis, M. (2015) Mycobacteria, metals, and the macrophage, *Immunol Rev 264*, 249-263 DOI 10.1111/imr.12265.

[5] Hood, M. I., and Skaar, E. P. (2012) Nutritional immunity: transition metals at the pathogen-host interface, *Nature reviews. Microbiology 10*, 525-537 DOI 10.1038/nrmicro2836.

[6] Schaible, U. E., and Kaufmann, S. H. (2004) Iron and microbial infection, *Nature reviews. Microbiology 2*, 946-953 DOI 10.1038/nrmicro1046.

[7] White, C., Lee, J., Kambe, T., Fritsche, K., and Petris, M. J. (2009) A role for the ATP7A copper-transporting ATPase in macrophage bactericidal activity, *J Biol Chem 284*, 33949-33956 DOI 10.1074/jbc.M109.070201.

[8] Rowland, J. L., and Niederweis, M. (2012) Resistance mechanisms of Mycobacterium tuberculosis against phagosomal copper overload, *Tuberculosis 92*, 202-210 DOI 10.1016/j.tube.2011.12.006.

[9] Wagner, D., Maser, J., Lai, B., Cai, Z., Barry, C. E., 3rd, Honer Zu Bentrup, K., Russell, D. G., and Bermudez, L. E. (2005) Elemental analysis of Mycobacterium avium-, Mycobacterium tuberculosis-, and Mycobacterium smegmatis-containing phagosomes indicates pathogen-induced microenvironments within the host cell's endosomal system, *Journal of immunology 174*, 1491-1500 DOI https://doi.org/10.4049/jimmunol.174.3.1491.

[10] Ward, S. K., Abomoelak, B., Hoye, E. A., Steinberg, H., and Talaat, A. M. (2010) CtpV: a putative copper exporter required for full virulence of Mycobacterium tuberculosis, *Mol Microbiol 77*, 1096-1110 DOI 10.1111/j.1365-2958.2010.07273.x.

[11] Wolschendorf, F., Ackart, D., Shrestha, T. B., Hascall-Dove, L., Nolan, S., Lamichhane, G., Wang, Y., Bossmann, S. H., Basaraba, R. J., and Niederweis, M. (2011) Copper resistance is essential for virulence of Mycobacterium tuberculosis, *Proc Natl Acad Sci U S A 108*, 1621-1626 DOI 10.1073/pnas.1009261108.

[12] Gold, B., Deng, H., Bryk, R., Vargas, D., Eliezer, D., Roberts, J., Jiang, X., and Nathan, C. (2008) Identification of a copper-binding metallothionein in pathogenic mycobacteria, *Nature chemical biology 4*, 609-616 DOI 10.1038/nchembio.109.

[13] Rowland, J. L., and Niederweis, M. (2013) A multicopper oxidase is required for copper resistance in Mycobacterium tuberculosis, *J Bacteriol 195*, 3724-3733 DOI 10.1128/jb.00546-13.

[14] Speer, A., Shrestha, T. B., Bossmann, S. H., Basaraba, R. J., Harber, G. J., Michalek, S. M., Niederweis, M., Kutsch, O., and Wolschendorf, F. (2013) Copper-boosting compounds: a novel concept for antimycobacterial drug discovery, *Antimicrobial agents and chemotherapy 57*, 1089-1091 DOI 10.1128/AAC.01781-12.

[15] Shah, S., Dalecki, A. G., Malalasekera, A. P., Crawford, C. L., Michalek, S. M., Kutsch, O., Sun, J., Bossmann, S. H., and Wolschendorf, F. (2016) 8-Hydroxyquinolines Are Boosting Agents of Copper-Related Toxicity in Mycobacterium tuberculosis, *Antimicrobial agents and chemotherapy 60*, 5765-5776 DOI 10.1128/AAC.00325-16.

[16] Dalecki, A. G., Haeili, M., Shah, S., Speer, A., Niederweis, M., Kutsch, O., and Wolschendorf, F. (2015) Disulfiram and Copper Ions Kill Mycobacterium tuberculosis in a Synergistic Manner, *Antimicrobial agents and chemotherapy 59*, 4835-4844 DOI 10.1128/AAC.00692-15.

[17] Tyagi, P., Dharmaraja, A. T., Bhaskar, A., Chakrapani, H., and Singh, A. (2015) Mycobacterium tuberculosis has diminished capacity to counteract redox stress induced by elevated levels of endogenous superoxide, *Free Radic Biol Med 84*, 344-354 DOI 10.1016/j.freeradbiomed.2015.03.008.

[18] Vilcheze, C., Hartman, T., Weinrick, B., and Jacobs, W. R., Jr. (2013) Mycobacterium tuberculosis is extraordinarily sensitive to killing by a vitamin C-induced Fenton reaction, *Nat Commun 4*, 1881 DOI 10.1038/ncomms2898.

[19] Grant, S. S., Kaufmann, B. B., Chand, N. S., Haseley, N., and Hung, D. T. (2012) Eradication of bacterial persisters with antibiotic-generated hydroxyl radicals, *Proc Natl Acad Sci U S A 109*, 12147-12152 DOI 10.1073/pnas.1203735109.

[20] Palde, P. B., Bhaskar, A., Pedro Rosa, L. E., Madoux, F., Chase, P., Gupta, V., Spicer, T., Scampavia, L., Singh, A., and Carroll, K. S. (2016) First-in-Class Inhibitors of Sulfur Metabolism with Bactericidal Activity against Non-Replicating M. tuberculosis, *ACS chemical biology 11*, 172-184 DOI 10.1021/acschembio.5b00517.

[21] Mishra, S., Shukla, P., Bhaskar, A., Anand, K., Baloni, P., Jha, R. K., Mohan, A., Rajmani, R. S., Nagaraja, V., Chandra, N., and Singh, A. (2017) Efficacy of beta-lactam/beta-lactamase inhibitor combination is linked to WhiB4-mediated changes in redox physiology of Mycobacterium tuberculosis, *Elife 6* DOI 10.7554/eLife.25624.

[22] Singh, R., Manjunatha, U., Boshoff, H. I., Ha, Y. H., Niyomrattanakit, P., Ledwidge, R., Dowd, C. S., Lee, I. Y., Kim, P., Zhang, L., Kang, S., Keller, T. H., Jiricek, J., and Barry, C. E., 3rd. (2008) PA-824 kills nonreplicating Mycobacterium tuberculosis by intracellular NO release, *Science 322*, 1392-1395 DOI 10.1126/science.1164571.

[23] Jin, Y., Lewis, M. A., Gokhale, N. H., Long, E. C., and Cowan, J. A. (2007) Influence of stereochemistry and redox potentials on the single- and double-strand DNA cleavage efficiency of Cu(II) and Ni(II) Lys-Gly-His-derived ATCUN metallopeptides, *J Am Chem Soc 129*, 8353-8361 DOI 10.1021/ja0705083.

[24] Libardo, M. D., Gorbatyuk, V. Y., and Angeles-Boza, A. M. (2016) Central Role of the Copper-Binding Motif in the Complex Mechanism of Action of Ixosin: Enhancing Oxidative Damage and Promoting Synergy with Ixosin B, *ACS Infect Dis 2*, 71-81 DOI 10.1021/acsinfecdis.5b00140.

[25] Libardo, M. D. J., Bahar, A. A., Ma, B., Fu, R., McCormick, L. E., Zhao, J., McCallum, S. A., Nussinov, R., Ren, D., Angeles-Boza, A. M., and Cotten, M. L. (2017) Nuclease activity gives an edge to host-defense peptide piscidin 3 over piscidin 1, rendering it more effective against persisters and biofilms, *FEBS J 284*, 3662-3683 DOI 10.1111/febs.14263.

[26] Libardo, M. D., Paul, T. J., Prabhakar, R., and Angeles-Boza, A. M. (2015) Hybrid peptide ATCUN-sh-Buforin: Influence of the ATCUN charge and stereochemistry on antimicrobial activity, *Biochimie 113*, 143-155 DOI 10.1016/j.biochi.2015.04.008.

[27] Libardo, M. D., Cervantes, J. L., Salazar, J. C., and Angeles-Boza, A. M. (2014) Improved bioactivity of antimicrobial peptides by addition of amino-terminal copper and nickel (ATCUN) binding motifs, *ChemMedChem 9*, 1892-1901 DOI 10.1002/cmdc.201402033.

[28] Park, C. B., Yi, K. S., Matsuzaki, K., Kim, M. S., and Kim, S. C. (2000) Structure-activity analysis of buforin II, a histone H2A-derived antimicrobial peptide: the proline hinge is responsible for the cell-penetrating ability of buforin II, *Proc Natl Acad Sci U S A 97*, 8245-8250 10.1073/pnas.150518097.

[29] Brewer, G. J. (2009) Zinc and tetrathiomolybdate for the treatment of Wilson's disease and the potential efficacy of anticopper therapy in a wide variety of diseases, *Metallomics 1*, 199-206 DOI 10.1039/b901614g.

[30] Bhaskar, A., Chawla, M., Mehta, M., Parikh, P., Chandra, P., Bhave, D., Kumar, D., Carroll, K. S., and Singh, A. (2014) Reengineering redox sensitive GFP to measure mycothiol redox potential of

Mycobacterium tuberculosis during infection, *PLoS Pathog 10*, e1003902 DOI 10.1371/journal.ppat.1003902.

[31] Ravindra Kumar, S., and Imlay, J. A. (2013) How Escherichia coli tolerates profuse hydrogen peroxide formation by a catabolic pathway, *J Bacteriol 195*, 4569-4579 DOI 10.1128/JB.00737-13.

[32] Slauch, J. M. (2011) How does the oxidative burst of macrophages kill bacteria? Still an open question, *Mol Microbiol 80*, 580-583 DOI 10.1111/j.1365-2958.2011.07612.x.

[33] Koivusalo, M., Welch, C., Hayashi, H., Scott, C. C., Kim, M., Alexander, T., Touret, N., Hahn, K. M., and Grinstein, S. (2010) Amiloride inhibits macropinocytosis by lowering submembranous pH and preventing Rac1 and Cdc42 signaling, *The Journal of Cell Biology 188*, 547-563 DOI 10.1083/jcb.200908086.

[34] Zeng, L., Miller, E. W., Pralle, A., Isacoff, E. Y., and Chang, C. J. (2006) A selective turn-on fluorescent sensor for imaging copper in living cells, *J Am Chem Soc 128*, DOI 10-11 10.1021/ja055064u.

[35] Vandal, O. H., Pierini, L. M., Schnappinger, D., Nathan, C. F., and Ehrt, S. (2008) A membrane protein preserves intrabacterial pH in intraphagosomal Mycobacterium tuberculosis, *Nat Med 14*, 849-854 DOI 10.1038/nm.1795.

[36] Boyer, E., Bergevin, I., Malo, D., Gros, P., and Cellier, M. F. M. (2002) Acquisition of Mn(II) in Addition to Fe(II) Is Required for Full Virulence of Salmonella enterica Serovar Typhimurium, *Infection and immunity 70*, 6032-6042 DOI 10.1128/IAI.70.11.6032-6042.2002.

[37] Svenson, J., Brandsdal, B. O., Stensen, W., and Svendsen, J. S. (2007) Albumin binding of short cationic antimicrobial micropeptides and its influence on the in vitro bactericidal effect, *J Med Chem 50*, 3334-3339 DOI 10.1021/jm0703542.

[38] Torrico, M., Aguilar, L., Sevillano, D., Gimenez, M. J., Alou, L., Gonzalez, N., Cafini, F., Cleeland, R., and Prieto, J. (2011) Activity of simulated serum concentrations of daptomycin versus vancomycin during the first 24h of treatment in the presence of physiological albumin concentrations against vancomycin-susceptible, -tolerant or -intermediate-resistant Staphylococcus aureus, *International journal of antimicrobial agents 37*, 332-338 DOI 10.1016/j.ijantimicag.2010.12.007.

[39] Dalhoff, A. (2018) Seventy-Five Years of Research on Protein Binding, *Antimicrobial agents and chemotherapy 62* DOI 10.1128/AAC.01663-17.

[40] Wang, C., Zhao, G., Wang, S., Chen, Y., Gong, Y., Chen, S., Xu, Y., Hu, M., Wang, X., Zeng, H., Wang, A., Liu, D., Su, Y., Cheng, T., Chen, F., and Wang, J. (2018) A Simplified Derivative of Human Defensin 5 with Potent and Efficient Activity against Multidrug-Resistant Acinetobacter baumannii, *Antimicrobial agents and chemotherapy 62* DOI 10.1128/AAC.01504-17.

[41] Patel, Y. S., and Mehra, S. (2017) Synergistic Response of Rifampicin with Hydroperoxides on Mycobacterium: A Mechanistic Study, *Frontiers in microbiology 8*, 2075 DOI 10.3389/fmicb.2017.02075.

[42] Vilcheze, C., Hartman, T., Weinrick, B., Jain, P., Weisbrod, T. R., Leung, L. W., Freundlich, J. S., and Jacobs, W. R., Jr. (2017) Enhanced respiration prevents drug tolerance and drug resistance in Mycobacterium tuberculosis, *Proc Natl Acad Sci U S A 114*, 4495-4500 DOI 10.1073/pnas.1704376114.

[43] Piccaro, G., Pietraforte, D., Giannoni, F., Mustazzolu, A., and Fattorini, L. (2014) Rifampin induces hydroxyl radical formation in Mycobacterium tuberculosis, *Antimicrobial agents and chemotherapy 58*, 7527-7533 DOI 10.1128/AAC.03169-14.

[44] Campbell, E. A., Korzheva, N., Mustaev, A., Murakami, K., Nair, S., Goldfarb, A., and Darst, S. A. (2001) Structural mechanism for rifampicin inhibition of bacterial rna polymerase, *Cell 104*, 901-912 DOI https://doi.org/10.1016/S0092-8674(01)00286-0.

[45] Darwin, K. H. (2015) Mycobacterium tuberculosis and Copper: A Newly Appreciated Defense against an Old Foe?, *J Biol Chem 290*, 18962-18966 DOI 10.1074/jbc.R115.640193.

[46] Porcheron, G., Garenaux, A., Proulx, J., Sabri, M., and Dozois, C. M. (2013) Iron, copper, zinc, and manganese transport and regulation in pathogenic Enterobacteria: correlations between strains, site of infection and the relative importance of the different metal transport systems for virulence, *Front Cell Infect Microbiol 3*, 90 DOI 10.3389/fcimb.2013.00090.

[47] Dwyer, D. J., Belenky, P. A., Yang, J. H., MacDonald, I. C., Martell, J. D., Takahashi, N., Chan, C. T., Lobritz, M. A., Braff, D., Schwarz, E. G., Ye, J. D., Pati, M., Vercruysse, M., Ralifo, P. S., Allison, K. R., Khalil, A. S., Ting, A. Y., Walker, G. C., and Collins, J. J. (2014) Antibiotics induce redox-related physiological alterations as part of their lethality, *Proc Natl Acad Sci U S A 111*, E2100-2109 DOI 10.1073/pnas.1401876111.

[48] Kohanski, M. A., Dwyer, D. J., Hayete, B., Lawrence, C. A., and Collins, J. J. (2007) A common mechanism of cellular death induced by bactericidal antibiotics, *Cell 130*, 797-810 DOI 10.1016/j.cell.2007.06.049.

[49] Kuhnert, N. (2013) One size does not fit all--bacterial cell death by antibiotics cannot be explained by the action of reactive oxygen species, *Angew Chem Int Ed Engl 52*, 10946-10948 DOI 10.1002/anie.201304548.

[50] Liu, Y., and Imlay, J. A. (2013) Cell death from antibiotics without the involvement of reactive oxygen species, *Science 339*, 1210-1213 DOI 10.1126/science.1232751.

[51] Elwell, C. E., Gagnon, N. L., Neisen, B. D., Dhar, D., Spaeth, A. D., Yee, G. M., and Tolman, W. B. (2017) Copper-Oxygen Complexes Revisited: Structures, Spectroscopy, and Reactivity, *Chem Rev 117*, 2059-2107 DOI 10.1021/acs.chemrev.6b00636.

[52] Haas, K. L., Putterman, A. B., White, D. R., Thiele, D. J., and Franz, K. J. (2011) Model peptides provide new insights into the role of histidine residues as potential ligands in human cellular copper acquisition via Ctr1, *J Am Chem Soc 133*, 4427-4437 DOI 10.1021/ja108890c.

[53] Rozga, M., Sokolowska, M., Protas, A. M., and Bal, W. (2007) Human serum albumin coordinates Cu(II) at its N-terminal binding site with 1 pM affinity, *Journal of biological inorganic chemistry : JBIC : a publication of the Society of Biological Inorganic Chemistry 12*, 913-918 DOI 10.1007/s00775-007-0244-8.

[54] Achard, M. E., Stafford, S. L., Bokil, N. J., Chartres, J., Bernhardt, P. V., Schembri, M. A., Sweet, M. J., and McEwan, A. G. (2012) Copper redistribution in murine macrophages in response to Salmonella infection, *The Biochemical journal 444*, 51-57 DOI 10.1042/bj20112180.

[55] Alberts, B., Johnson, A., Lewis, J., Raff, M., Roberts, K., and Walter, P. (2008) Intracellular Compartments and Protein Sorting, In *Molecular biology of the cell* (Anderson, M., and Granum, S., Eds.) 5th ed., pp 695-748, Garland Science, Taylor & Francis Group, LLC, New York, NY.

[56] Olakanmi, O., Schlesinger, L. S., Ahmed, A., and Britigan, B. E. (2002) Intraphagosomal Mycobacterium tuberculosis acquires iron from both extracellular transferrin and intracellular iron pools. Impact of interferon-gamma and hemochromatosis, *J Biol Chem 277*, 49727-49734 DOI 10.1074/jbc.M209768200.

TOC Graphic

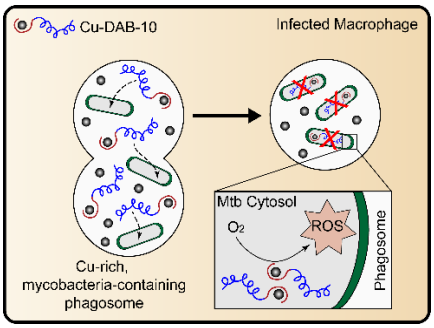
Cu-DAB-10
Infected Macrophage
Mtb Cytosol
O2
ROS
Phagosome
Cu-rich,
mycobacteria-containing
phagosome

Synopsis

The designed peptidomimetic induces a copper hypersensitivity phenotype in Mycobacterium tuberculosis.